Third International Conference on CFD in the Minerals and Process Industries
CSIRO, Melbourne, Australia
10-12 December 2003

FLOW MODELING FOR DESIGN OF CARBOTHERMIC ALUMINIUM REACTORS

Dimitrios I. GEROGIORGIS and B. Erik YDSTIE

Department of Chemical Engineering, Carnegie Mellon University, Pittsburgh, Pennsylvania, PA 15213, USA

ABSTRACT

The present simulation study elaborates on a CFD model (Gerogiorgis et al., 2003) developed for the second stage of a conceptual carbothermic aluminium reactor design which is specifically aimed at industrial implementation. Carbothermic production of aluminium is an alternative to the conventional Hall-Héroult electrolysis process and is characterized by cost and environmental advantages, but also by unique chemistry and challenging complexity [1].

A detailed two-dimensional CFD model of the core stage of a proposed carbothermic aluminium reactor design has been constructed in order to analyze and understand the steady state operation of an industrial scale reactor and the interplay among electric heating, conduction, convection, chemical reaction and turbulent flow within its core stage. The corresponding steady state triple PDE problem (electric charge, heat and momentum balances) for the slag flow in the core reactor stage has been solved using the finite element method with quadratic basis functions in a commercial CFD simulation environment (FEMLAB® 2.3) to obtain potential, temperature and velocity distributions.

Modeling the interaction among heat production (Joule heating effect), heat consumption (endothermic reaction) and turbulent flow (significantly high Reynolds numbers) is of paramount importance for improving the performance of the core stage of the carbothermic aluminium reactor. The objective of this study is to extract conclusions so as to provide reactor design guidelines and recommendations.

NOMENCLATURE

V	electric field potential	[V]
E	electric field intensity	$[V.m^{-1}]$
T	temperature	[K]
U	slag velocity	$[m.s^{-1}]$
P	pressure	[Pa]
ρ	density	$[kg.m^{-3}]$
μ	dynamic viscosity	$[kg.m^{-1}.s^{-1}]$
σ	electrical conductivity	$[Ohm^{-1}.m^{-1}]$
k	thermal conductivity	$[W. m^{-1}.K^{-1}]$
C_P	const. pressure spec. heat capacity	$[J.mol^{-1}.K^{-1}]$
k_0	preexponential reaction rate factor	$[mol.m^{-3}.s^{-1}]$
ΔH	carbothermic reaction enthalpy	$[J.mol^{-1}]$
ΔG	carbothermic reaction free energy	$[J.mol^{-1}.K^{-1}]$
k	turbulent kinetic energy	$[m^2.s^{-2}]$
ε	dissipation energy	$[m^2.s^{-3}]$
C_μ	turbulent viscosity constant	[0.09]
$C_{\varepsilon 1}$	turbulent viscosity constant	[0.1256]
$C_{\varepsilon 2}$	turbulent viscosity constant	[1.92]
σ_ε	dissipation equation ε constant	[1.3]
σ_k	dissipation equation constant	[1.0]

INTRODUCTION

Carbothermic reduction is the only non-electrochemical process proposed and tested for aluminium production [2]. The high reaction temperatures still entail electric heating, but a carbothermic process is more energy efficient and has a remarkably high theoretical volumetric productivity [2]. Thus, considerable industrial implementation advantages can be achieved and economies of scale can be realized. The interest in carbothermic reactor technology is driven by significant cost advantages in both largest cost sectors: **(a)** an identified potential for capital investment reduction due to higher reactor productivity and lower maintenance requirements than those of electrochemical processes [3]. **(b)** a significant potential for higher energy efficiency which can be achieved by utilizing C and CO off-gases as useful energy sources for electric power cogeneration [4].

Nevertheless, carbothermic reduction of aluminium oxide is also remarkably complicated for many different reasons: **(a)** Aluminium carbide formation is thermodynamically favored at temperatures below aluminium formation; thus, Al_4C_3 is a key intermediate species that affects balances, chemical equilibrium and hence overall conversion [2-4]. **(b)** Process temperatures are required to be extremely high (exceeding 1900 °C in melting and 2100 °C in reduction), resulting in major radiation heat losses for most designs; efficient heat integration is equally important for technical feasibility and economic viability of industrial processes. **(c)** Carbon monoxide (CO) is the overall gaseous product. Greenhouse gas emissions raise environmental concerns; however, energy recovery is possible via heat exchange and subsequent combustion for power cogeneration [2, 4]. **(d)** Al has a high vapor pressure and evaporates readily at the reaction temperatures under atmospheric pressure; this is also aggravated by a tendency for vapor Al_2O formation.

Carbothermic reduction can be a two-stage process [5], and it is based on a complicated, reversible, multiphase and multi-species chemical reaction phenomenon [2, 4, 6-9]. The actual reaction mechanism has not been elucidated, but ionic species identification has been conducted [4] and there is a reaction rate model proposed by Frank et al. [7]; the reactants are aluminium oxide (Al_2O_3) and carbon (C), key reaction intermediates are aluminium suboxide (Al_2O) and aluminium carbide (Al_4C_3), and the end products are molten aluminium (Al) and carbon monoxide (CO): the complexity is illustrated by this simultaneous coexistence of solids and gases in the multicomponent reactive slag. Carbon in various forms has been tested and proposed as a reducing agent in many previous experimental studies conducted at laboratory and pilot plant scale [4, 7-9]. Several process pathways and reactor configurations have been proposed and tested for commercialization [4, 5, 10].

CARBOTHERMIC REACTOR ENGINEERING

A variety of industrial-scale reactor designs have been proposed in the patent literature over the last 40 years [4]; complexity has evolved with advances in understanding. The Advanced Reactor Process (ARP) is based on the carbothermic reactor patent of Johansen and Aune [11]; a detailed schematic of this reactor is provided in Figure 1 (flowsheet unit numbers correspond to patent descriptions). The effort to take advantage of chemistry by separating phenomena in four distinct stages (**2**, **3**, **10**, **44**) is obvious:

1. The *first stage* is the **pre-reduction smelting zone**. Carbon and aluminium oxide pellets are continuously fed to a submerged arc smelter, melt, react and form a molten slag contained in a inert-atmosphere, oil-cooled reactor. The reaction of aluminium oxide with excess of carbon to form the Al_4C_3-rich slag of the first stage is (T > 1900 °C):

$$2Al_2O_{3(s)} + 9C_{(s)} \rightarrow (Al_4C_3+Al_2O_3)_{(slag)} + 6CO_{(g)} \qquad (1)$$

2. The *second stage* is a **high-temperature reaction zone**: the first-stage molten slag flows into this core stage (a multi-electrode, high-temperature submerged arc reactor); the slag is heated to a higher temperature, avoiding severe local surface superheating caused in open arc reactors. Liquid Al droplets and CO bubbles are rapidly generated, with concurrent Al_4C_3 injection to avoid carbon depletion. The decomposition of the first-stage, Al_4C_3-rich slag to form the second-stage, Al-rich phase is (T > 2000 °C):

$$(Al_4C_3 + Al_2O_3)_{(slag)} \rightarrow (6Al + Al_4C_3)_{(metal)} + 3CO_{(g)} \qquad (2)$$

3. The *third stage* is a **vapor recovery reactor (VRR)**, where Al and Al_2O vapors react with C to form Al_4C_3. Vaporization occurs as CO vapors sweep the second stage: unless $Al_{(g)}$ is recovered countercurrent to incoming solid feed, metal losses are catastrophic for process economics. Undesirable vaporization is thus reduced by staging and feeding the first and second stage gas streams to the VRR. The recovered Al_4C_3 (recycle stream) is reinjected into the reactor, minimizing Al emissions and maximizing yield. Countercurrent flow exceeds incoming reactant preheating needs, thus allowing for energy recovery via cogeneration.
4. The *fourth stage* of the process is the **purification zone**: liquid aluminium flows through an overflow weir to an aluminium metal separation unit, where entrained $Al_4C_{3(s)}$ and dissolved $C_{(s)}$ are removed via proprietary technology.

MODELING: REASONS AND OBJECTIVES

The present study concentrates on understanding the effect of conceptual design decisions on state variable profiles, using a two-dimensional model of the core (second) stage. Prior experience identifies technical challenges anticipated for industrial implementation of carbothermic technology, and relevant reports highlight the problems [4-5, 10-12]. The first-principle CFD modeling endeavor undertaken by the Department of Chemical Engineering and CAPD at Carnegie Mellon University is only part of a coordinated multidisciplinary effort aimed at enhanced understanding of carbothermic reduction technology and reactor design. This challenging process research and development (R&D) effort has been presented in our previous publication [13], as has been done with the concept of the ARP reactor [14] and the economic evaluation of a potential venture [15].

One of the strategic objectives of this collaborative effort is to precisely understand the flow and reaction behavior of the molten slag within the carbothermic aluminium reactor, but also the interaction among AC electrode slag heating, Joule heat production, reaction heat consumption, conductive and convective heat transport, and turbulence. Process design efficiency and optimality are important, given: **(a)** this is a high-temperature metallurgical process, **(b)** heat integration is a necessity for economic feasibility, **(c)** the inert gas atmosphere is essential for safe operation, **(d)** suitable manipulation variables are exceptionally few, and **(e)** the observable characteristic times are very long.

The foregoing facts highlight the importance of modeling, because the ongoing experimental campaign efforts [14] can significantly benefit from modeling recommendations, the goal being to expedite R&D and commercialization. The strategic objective of computationally modeling and understanding heat transfer and flow in this electrothermic reactor addresses effectively the above five challenges and can further enhance our conceptual reactor design intuition. Thermophysical property compilation and modeling and preliminary 3D electrothermic modeling are essential and parameter values used are taken from our prior work [16]; moreover, we have pursued integrated PDE flow modeling under the assumption of laminar Navier-Stokes flow [17]. Recently, a first-principle MINLP optimization model has been proposed for efficient electrode heating design [18].

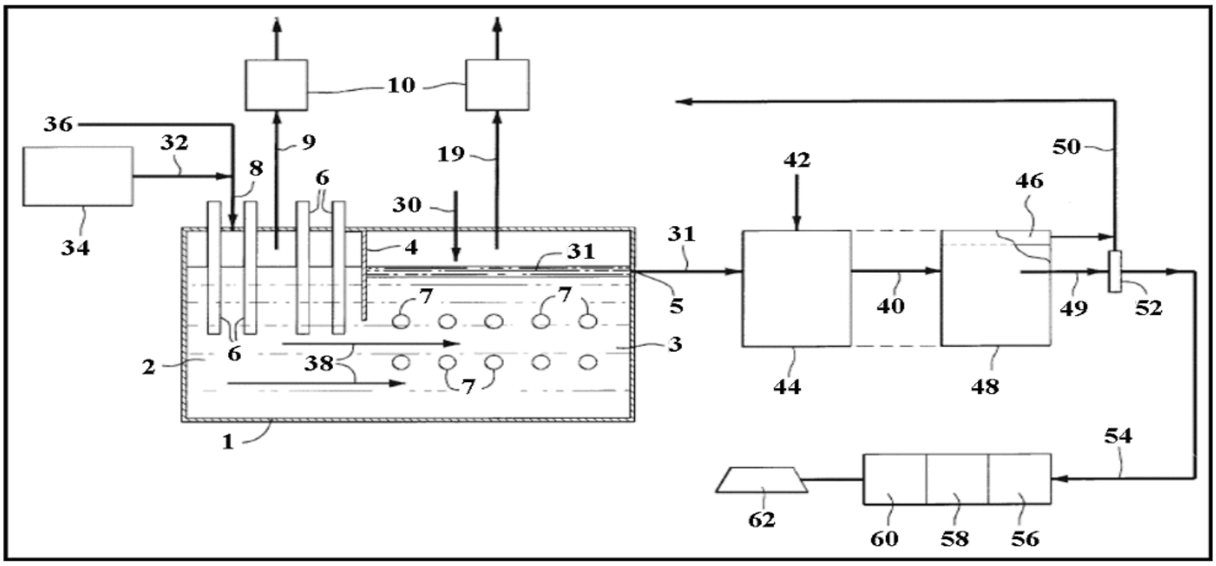

Figure 1: Schematic of a proposed carbothermic aluminium reactor according to the Advanced Reactor Process (ARP) [11].

MODEL DESCRIPTION

The multielectrode second stage of a carbothermic reactor is modeled considering the complete two-dimensional section perpendicular to the reactor axis at a vertical plane defined by the horizontal electrode circular tips (Figure 2). The resulting two-dimensional computational domain comprises a molten slag reservoir, an underflow inlet duct and the complete second stage of the reactor, considering multiple graphite electrode tips immersed in a liquid slag.

The full reactor and homogeneous slag assumptions are used in order to simplify the many physical phenomena and study electric charge, heat and momentum balances. The goal here is to solve the steady state PDE problems for the respective variables of these three balances [potential (V), field intensity (E), temperature (T), velocity (U_x ,U_y), pressure (P)], obtaining reliable starting points so as to solve molar balances for species concentration profiles in a complete model reliable for performance evaluation. Constant thermophysical properties are assumed and have been estimated using the correlations published in [16], except for a temperature-dependent electric conductivity that has been used to illustrate the strong coupling between the charge balance and the Joule heat generation term [16]. The standard k-ε model of Launder and Spalding (1972) described by Chung [19] is used in the momentum balance to analyze the turbulent slag flow inside the ARP reactor.

The resulting finite element CFD model of the reactor has been solved with quadratic finite element basis functions on a fine unstructured triangular grid (12,124 elements), using commercial simulation software (FEMLAB® v. 2.3). Three FEMLAB® multiphysics modules have been used and integrated for the simulations (Conductive Media DC, Convection and Conduction, and K-ε Turbulence Model). For the present case, nominal Reynolds numbers indicate slag flow well within the turbulent regime (Re ~ 30,000). The k-ε turbulence model equation constants selected correspond exactly to those recommended by Chung [19] and also used in published FEMLAB® model studies [20]. A preliminary stepwise procedure (one more PDE problem solved at a time) can be followed to successfully initialize the full problem and thus handle strong balance couplings, especially if parameter correlations implicitly dependent on state variables are to be used in the integrated simulations. A crucial goal considered and a perspective maintained in this study is the upcoming augmentation of the model, in order to handle molar species concentration calculations, and the routine simultaneous solution of coupled PDE balances, that will render it a suitable process design tool.

CFD EQUATIONS AND BOUNDARY CONDITIONS

The steady state CFD problem considered in this paper comprises three PDE balances and the corresponding partial differential equations on a two-dimensional domain. The first part is the steady state electric charge balance:

$$\nabla^2 V = V_{xx} + V_{yy} = 0 \tag{3}$$

The second part is the steady state heat balance:

$$\nabla \cdot (k\nabla T - \rho C_P T\mathbf{U}) + \sigma(\nabla V)^2 - k_0 \exp\left(\frac{-\Delta G}{RT}\right)\Delta H = 0 \tag{4}$$

The third part is the steady state momentum balance:

$$\rho(\mathbf{U}\cdot\nabla\mathbf{U}) - \nabla\cdot\left[\left(\mu + \rho\frac{C_\mu}{\sigma_k}\frac{k^2}{\varepsilon}\right)\cdot\left(\nabla\mathbf{U} + (\nabla\mathbf{U})^T\right)\right] = -\nabla P \tag{5}$$

which also comprises the incompressible continuity PDE:

$$\nabla\cdot\mathbf{U} = 0 \tag{6}$$

complemented with the two standard k-ε model equations:

$$\rho(\mathbf{U}\cdot\nabla k) - \nabla\cdot\left[\left(\mu + \rho\frac{C_\mu}{\sigma_k}\frac{k^2}{\varepsilon}\right)\nabla k\right] = \rho C_\mu \frac{k^2}{\varepsilon}\left(\nabla\mathbf{U} + (\nabla\mathbf{U})^T\right)^2 - \rho\varepsilon \tag{7}$$

$$\rho(\mathbf{U}\cdot\nabla\varepsilon) - \nabla\cdot\left[\left(\mu + \rho\frac{C_\mu}{\sigma_\varepsilon}\frac{k^2}{\varepsilon}\right)\nabla\varepsilon\right] = \rho C_{\varepsilon 1} C_\mu k\left(\nabla\mathbf{U} + (\nabla\mathbf{U})^T\right)^2 - \rho C_{\varepsilon 2}\frac{\varepsilon^2}{k} \tag{8}$$

The imposed voltages on electrode tips (V_i , i=1-6) are set, zero voltage is used on both long horizontal domain sides to approximate the potential in the third lateral dimension, and zero gradient (∇V = 0) is used on all other wall sides, to account for the insulating behavior of solidified slag. Inlet slag (2173 K) and wall (473 K) temperatures are set, and heat insulation (∇T = 0) is assumed at electrode tips. An inlet vertical slag velocity is assumed ($U_0 = 0.1$ m.s^{-1}), with a suitable wall function [20] on the walls and all tips. A slip boundary condition is used for the slag free surface and zero pressure has been assumed at the reactor outlet. Electrode voltage tuning is of great importance, governing field intensity and current density distribution, thus also affecting Joule heat generation and temperature profiles. Therefore, two different stepwise constant voltage profiles have been considered in the simulations to probe coupled heat generation, consumption and turbulent convection and hence provide recommendations for electrode placement. Elimination of Lorentz (field) and Boussinesq (buoyancy) forces from (5) is based on high-frequency AC electrode use and negligible heat expansion coefficient, respectively.

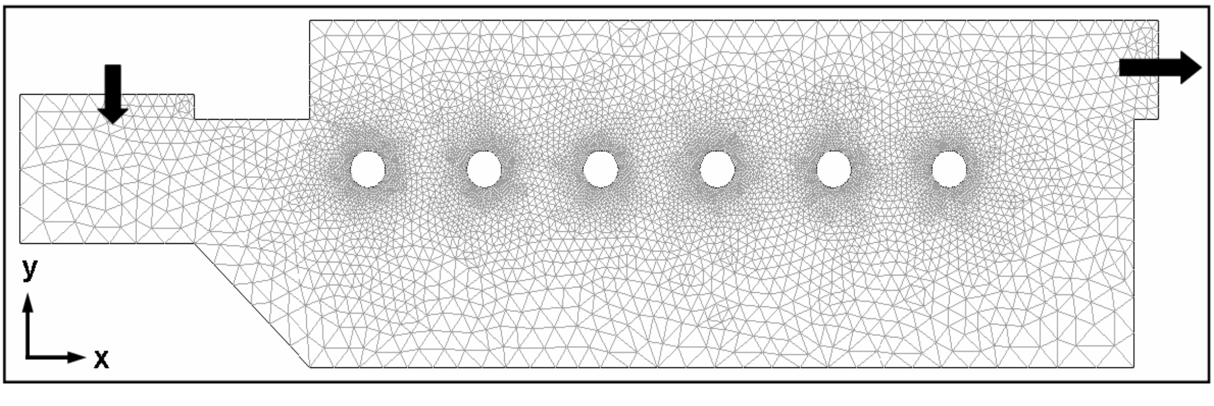

Figure 2: The two-dimensional computational domain and grid considered for CFD simulation of the carbothermic reactor.

CFD SIMULATION RESULTS: CASE 1 $V_1 = V_2 = V_3 = V_4 = V_5 = V_6 = 50$ V

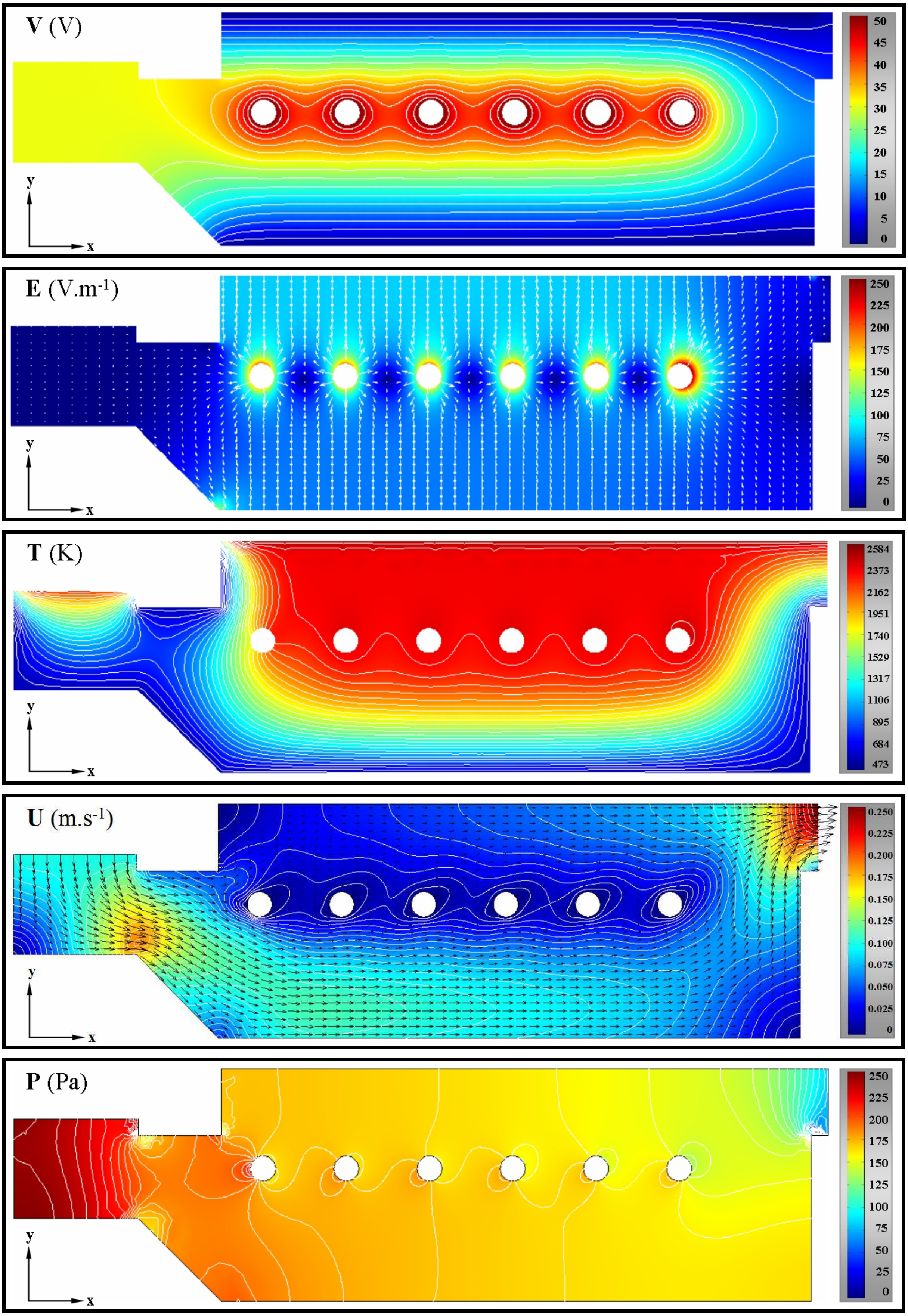

Figure 3: Electric potential (V), field intensity (E), temperature (T), velocity (**U**) and pressure (P) distribution - first case.

CFD SIMULATION RESULTS: CASE 2 $V_1 = V_2 = V_5 = V_6 = 50$ V , $V_3 = V_4 = 100$ V

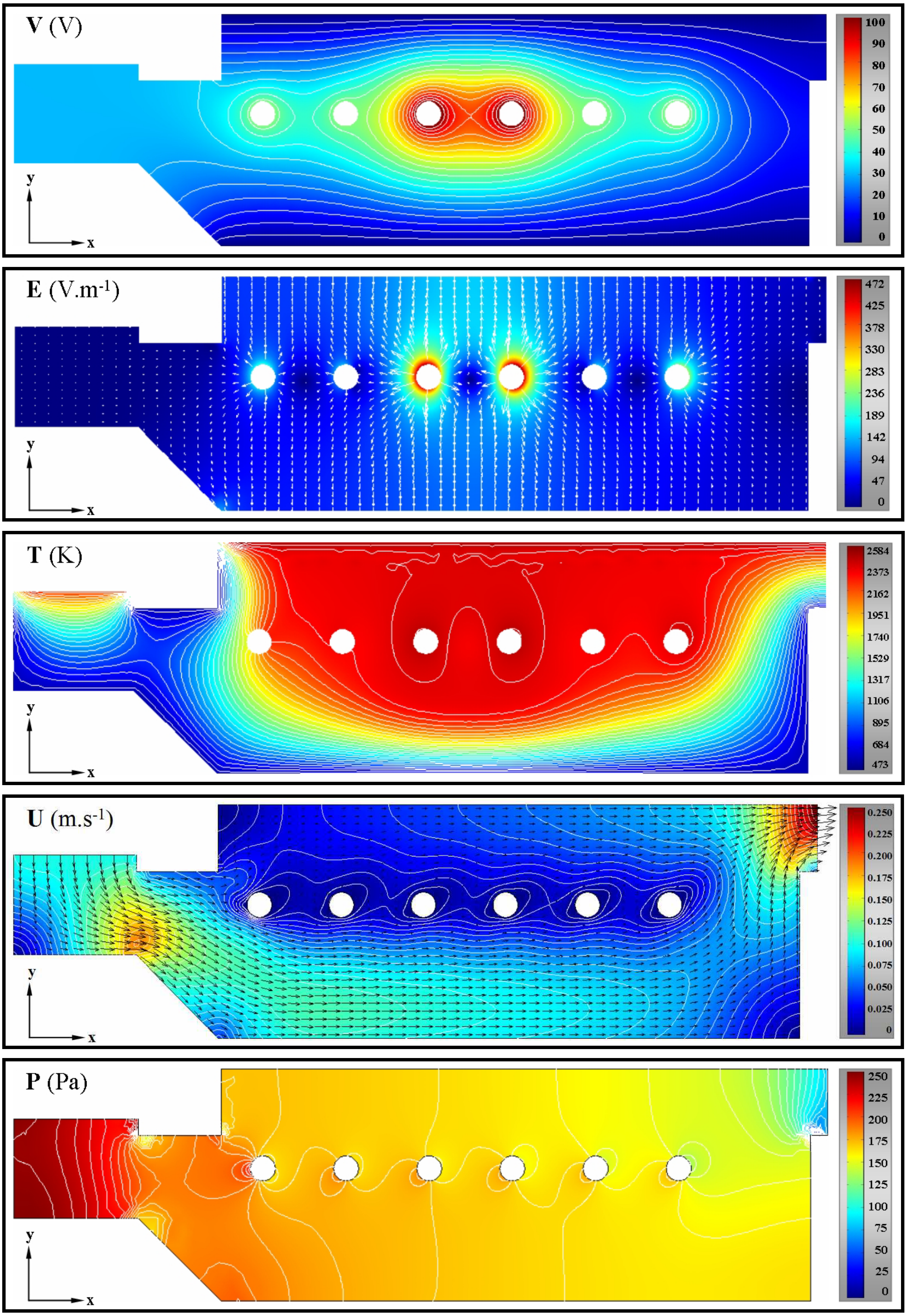

Figure 4: Electric potential (V), field intensity (E), temperature (T), velocity (**U**) and pressure (P) distributions - second case.

CONCLUSIONS

The present steady state multiphysics CFD modeling study uses a two-dimensional model of a carbothermic reactor to probe electric charge, heat and momentum balances in it. The major trends identified in analysis are the following: **(a)** The electric potential distribution is symmetric about the major horizontal axis of the reactor (electrode locus) and indicates certain polarization on the left slag reservoir, consistent with the presence of the first-stage electrodes; the zero-voltage assumption on horizontal sides compares well with previously obtained 3D simulation results [16]. **(b)** The field intensity distribution indicates in both cases a definite localization of electric activity and Joule heating close to the periphery of all the electrodes, although local minima are also evident on the line in between electrodes. **(c)** The temperature distribution is characterized by: (i) an extended, well-mixed, high-temperature reaction zone that is formed around the electrodes, and (ii) a cooled slag containment zone that is formed against the reactor walls. The presence of two higher voltage middle electrodes (second case) increases the reaction zone size appreciably and induces higher temperatures close to those electrodes, but the maximum temperature attained remains the same. **(d)** The velocity distribution indicates the presence of a rapid turbulent flow zone at the underflow contraction. The absence of laminar boundary layers is noticeable here, in contrast to previous results published for lower Re [17]. Moreover, circulation is substantial at the bottom part of the reactor, and convection domination therein reduces temperature considerably, in addition to external cooling. The significant size of this bottom circulation zone can be explained due to the turbulent kinetic energy dissipation. Design implications are obvious: the appreciable distance between the bottom flow and the electrode line indicates that the reactor depth is suboptimal and should be reduced. **(e)** The pressure distribution reveals rapid local drops in the underflow contraction and due to electrode presence. More sensitivity analyses with respect to crucial design variables can reveal reactor controllability margins [17]. Experimental validation is equally crucial, even if reliable high-temperature measurements are costly and laborious. Multiscale process modeling has also been proposed [21].

ACKNOWLEDGEMENTS

The authors acknowledge discussions and collaboration with M. Bruno and D. Roha (ALCOA Technical Center) as well as the financial support provided by ALCOA Inc. This study is part of a project co-funded by the U.S. Department of Energy (jointly undertaken by ALCOA Inc., ELKEM ASA Research and Carnegie Mellon University) for the detailed investigation of the technical feasibility and economic viability of carbothermic aluminium production. The first author (D.I.G.) hereby gratefully acknowledges a Fulbright fellowship awarded by the United States Department of State (Institute of International Education) as well as the honorary doctoral fellowship awarded by the Alexander S. Onassis Public Benefit Foundation of Greece.

REFERENCES

1. AUSTIN G.T., (1984), “Shreve’s Chemical Process Industries”; New York, NY (McGraw-Hill).
2. BURKIN A.R. (Ed.) (1987), “Production of Aluminium and Alumina”; New York, NY (Wiley).
3. WELCH, B.J. (1999), “Aluminium Production Paths in the New Millennium”; *JOM* **51**(5): 24.
4. MOTZFELDT, K., (1989), “Carbothermal Production of Aluminium”; Dusseldorf (Aluminium Verlag).
5. JOHANSEN, K., et al. (2000), “Carbothermic Aluminum”, in: *Proceedings of the Sixth International Conference on Molten Slags, Fluxes and Salts*” (paper #192); Stockholm, Sweden (CD edition).
6. QIU, C. and METSELAAR, R. (1995), “Thermodynamic Evaluation of the Al_2O_3-Al_4C_3 System”, *Z. Metallkd.* **86**(3), 198.
7. FRANK, R.A., FINN, C.W. and ELLIOTT, J.F., (1989), “Physical Chemistry of the Carbothermic Reduction of Alumina in the Presence of a Metallic Solvent: 2. Measurements of Kinetics of Reaction”, *Metall. Mater. Trans. B* **20**(2), 161.
8. FRANK, R.A. (1989), “Physical Chemistry of the Carbothermic Reduction of Alumina” (Ph.D. Thesis, Massachussetts Institute of Technology – Cambridge, MA).
9. KRAG, P.W. (1988), “On the Carbothermic Reduction of Anorthosite” (Ph.D. Thesis, Colorado School of Mines – Golden, CO).
10. SAAVEDRA, A.F. and KIBBY, R.M. (1988), “Investigating the Viability of Carbothermic Alumina Reduction”, *JOM* **40**(11): 32.
11. JOHANSEN, K. and AUNE, J. (2002), U.S. Patent 6,440,193 (assignees: ALCOA Inc. and ELKEM ASA).
12. KIBBY, R.M. and SAAVEDRA, A.F. (1987), “Model Studies in Carbothermic Reduction of Alumina”, in: ZABREZNIK, R.D. (Ed.): *Light Metals 1987*: 263; Warrendale, PA (TMS).
13. GEROGIORGIS, D.I., et al. (2003), “Process Systems Tools for Design and Optimization of Carbothermic Reduction Processes”, in: DAS, S.K. (Ed.), *Aluminium 2003*: 289; Warrendale, PA (TMS).
14. JOHANSEN, K., et al. (2003), “Aluminum Carbothermic Technology: ALCOA-ELKEM Advanced Reactor Process”, in: CREPEAU, P. (Ed.), *Light Metals 2003*: 401; Warrendale, PA (TMS).
15. BRUNO, M. (2003), “Aluminum Carbothermic Technology: Comparison to Hall-Héroult Process”, in: CREPEAU, P. (Ed.), *Light Metals 2003*: 395; Warrendale, PA (TMS).
16. GEROGIORGIS, D.I., YDSTIE, B.E. and SEETHARAMAN, S.S. (2002), “A Steady State Electrothermic Simulation Analysis of a Carbothermic Reduction Reactor for the Production of Aluminium”, in: CROSS, M., EVANS, J.W. and BAILEY, C. (Eds.), *Computational Modeling of Materials, Minerals, and Metals Processing*: 273; Warrendale, PA (TMS).
17. GEROGIORGIS, D.I. and YDSTIE, B.E. (2003), “A Finite Element CFD Sensitivity Analysis for the Conceptual Design of a Carbothermic Aluminium Reactor”, in: CREPEAU, P. (Ed.), *Light Metals 2003*: 407; Warrendale, PA (TMS).
18. GEROGIORGIS, D.I. and YDSTIE, B.E. (2003), “An MINLP Model for the Conceptual Design of a Carbothermic Aluminium Reactor”, in: *Proceedings of ESCAPE-13*: 131; (LUT, Lappeenranta, Finland).
19. CHUNG, T.J. (2002), “Computational Fluid Dynamics”; Cambridge, UK (Cambridge University Press).
20. FEMLAB® 2.3 Manual (Stockholm: COMSOL, 2002).
21. GEROGIORGIS, D.I. and YDSTIE, B.E. (2003), “A Multiscale Model for Design and Simulation of a Carbothermic Reduction Process for Aluminium Production”, in: *Proceedings of FOCAPO 2003*: 581; (Coral Springs, FL).